PPAR-γ Activation Restores Pancreatic Islet SERCA2 Levels and Prevents β-Cell Dysfunction under Conditions of Hyperglycemic and Cytokine Stress

Tatsuyoshi Kono, Geonyoung Ahn, Dan R. Moss, Liann Gann, Angel Zarain-Herzberg, Yurika Nishiki, Patrick T. Fueger, Takeshi Ogihara, and Carmella Evans-Molina

Departments of Medicine (T.K., D.R.M., C.E.-M.), Pediatrics (Y.N., P.T.F.) , and Cellular and Integrative Physiology (P.T.F., C.E.-M.), and the Herman B. Wells Center for Pediatric Research (G.A., L.G., Y.N., P.T.F., C.E.-M.), Indiana University School of Medicine, Indianapolis, Indiana 46202; Department of Biochemistry (A.Z.-H.), School of Medicine, National Autonomous University of México, Adpo Postal 70-159, México D.F. 04510; and Department of Metabolism and Endocrinology (T.O.), Juntendo University Graduate School of Medicine, Tokyo, 113-0033 Japan

The maintenance of intracellular Ca^{2+} homeostasis in the pancreatic β-cell is closely regulated by activity of the sarco-endoplasmic reticulum Ca^{2+} ATPase (SERCA) pump. Our data demonstrate a loss of β-cell SERCA2b expression in several models of type 2 diabetes including islets from db/db mice and cadaveric diabetic human islets. Treatment of 832/13 rat INS-1-derived cells with 25 mM glucose and the proinflammatory cytokine IL-1β led to a similar loss of SERCA2b expression, which was prevented by treatment with the peroxisome proliferator-activated receptor (PPAR)-γ agonist, pioglitazone. Pioglitazone was able to also protect against hyperglycemia and cytokine-induced elevations in cytosolic Ca^{2+} levels, insulin-secretory defects, and cell death. To determine whether PPAR-γ was a direct transcriptional regulator of the *SERCA2* gene, luciferase assays were performed and showed that a -259 bp region is sufficient to confer PPAR-γ transactivation; EMSA and chromatin immunoprecipitation experiments confirmed that PPAR-γ directly binds a PPAR response element in this proximal region. We next sought to characterize the mechanisms by which SERCA2b was down-regulated. INS-1 cells were exposed to high glucose and IL-1β in time course experiments. Within 2 h of exposure, activation of cyclin-dependent kinase 5 (CDK5) was observed and correlated with increased serine-273 phosphorylation of PPAR-γ and loss of SERCA2 protein expression, findings that were prevented by pioglitazone and roscovitine, a pharmacological inhibitor of CDK5. We conclude that pioglitazone modulates SERCA2b expression through direct transcriptional regulation of the gene and indirectly through prevention of CDK5-induced phosphorylation of PPAR-γ. **(*Molecular Endocrinology* 26: 257–271, 2012)**

Type 2 diabetes mellitus (T2DM) is a disease that is growing in epidemic proportions. Currently, nearly 26 million Americans have diabetes (1), and worldwide the number affected approaches 220 million. Given escalating rates of obesity and the global adoption of a Western lifestyle, this number is expected to double by 2030 (2). Recent emphasis has been placed on the role of the pancreatic β-cell in the comprehensive pathophysiology of T2DM (3, 4). Clinical and autopsy studies suggest that T2DM is characterized by a progressive loss of both β-cell function and mass (5–7). The diabetic milieu is enriched with high levels of glucose, pro-inflammatory cytokines,

ISSN Print 0888-8809 ISSN Online 1944-9917
Printed in U.S.A.

doi: 10.1210/me.2011-1181 Received July 13, 2011. Accepted December 14, 2011.
First Published Online January 12, 2012

Abbreviations: BMI, Body mass index; CDK5, cyclin-dependent kinase 5; CDKAL1, CDK5-regulatory subunit-associated protein1-like 1; ChIP, chromatin immunoprecipitation; DMSO, dimethylsulfoxide; ER, endoplasmic reticulum; GSIS, glucose-stimulated insulin secretion; HBSS, Hank's balanced salt solution; HG, high glucose; PPAR-γ, peroxisome proliferator-activated receptor γ; PPRE, PPAR-responsive element; qRT-PCR, quantitative RT-PCR; SERCA, sarco-endoplasmic reticulum Ca^{2+} ATPase; STZ, streptozotocin; T2DM, type 2 diabetes mellitus; UPR, unfolded protein response.

free fatty acids, and other lipid intermediates. These factors are directly toxic to the β-cell and activate several overlapping stress pathways including oxidative and endoplasmic reticulum (ER) stress, mitochondrial dysfunction, apoptosis, and necrosis (8–11).

Under normal conditions, the precise regulation of calcium (Ca^{2+}) homeostasis in the β-cell plays a key role in proinsulin processing, insulin-secretory function, and cellular survival (12). Glucose-stimulated insulin secretion (GSIS) from the pancreatic β-cell occurs through a Ca^{2+}-dependent mechanism that couples cellular depolarization with cytosolic Ca^{2+} influx from voltage-gated Ca^{2+} channels and insulin granule exocytosis (13–15). In addition to this central role in the secretory response, Ca^{2+} homeostasis is important in ER function, including protein folding and maturation (16, 17). A steep calcium concentration gradient is maintained across the cytosol to the ER lumen, where free Ca^{2+} is estimated to be at least 3 orders of magnitude higher than cytosolic Ca^{2+} levels (18–20). Alterations in ER Ca^{2+} levels directly impact chaperone activity and lead to activation of the unfolded protein response or UPR, a protective cascade aimed at limiting the delivery of new proteins to the ER (21). The UPR activates pathways that serve to slow global transcription and increase ER-folding capacity through enhanced transcription of molecular chaperones. If these protective maneuvers fail, however, continued activation of the UPR results in a state of ER stress and induction of an apoptotic program (8).

The sarco-ER Ca^{2+}-ATPase (SERCA) pump is positioned at the intersection of β-cell insulin production and secretion and ER health. The SERCA pump is a P-type ATPase that hydrolyzes one ATP molecule to move two Ca^{2+} molecules across the sarco- or ER membrane. The SERCA pumps are 110- to 115-kDa proteins consisting of 10–11 transmembrane helices, three cytoplasmic domains, an A or anchor domain, a P or phosphorylation domain, and an N domain where ATP binds (22). SERCA protein is encoded by one of three highly conserved genes: *SERCA* 1, 2, and 3. Alternative splicing at the carboxy terminus leads to a number of different SERCA isoforms, with 11 isoforms presently identified (23). The SERCA pump serves as an integral gatekeeper of ER function where its activity is responsible for maintaining high levels of Ca^{2+} within the ER lumen (24). Furthermore, after acute glucose stimulation and insulin granule exocytosis, SERCA activity is required to return basal cytosolic Ca^{2+} levels to prestimulation values (25).

Several groups have demonstrated that β-cell SERCA2 isoform b (SERCA2b) expression is decreased in selected models of diabetes (26–28). In addition, our group has previously shown that *in vivo* loss of SERCA2b mRNA in islets from C57BLKS/J-db/db mice, a strain lacking a functional leptin receptor, can be restored through systemic administration of a pharmacological agonist of the peroxisome proliferator-activated receptor γ (PPAR-γ) (26). To date, however, the underlying mechanisms and functional consequences of SERCA2b dysregulation have not been fully defined in pancreatic β-cells.

Here, we validate the observation that pancreatic islet SERCA2b expression is diminished in diabetes. Importantly, we show that SERCA2b expression is decreased in human islets isolated from cadaveric donors with T2DM. We further demonstrate that SERCA2b loss leads to alterations in insulin secretion and β-cell survival and show that PPAR-γ is a direct transcriptional regulator of the *SERCA2* gene, acting via a novel PPAR-responsive element (PPRE) in a key regulatory region −249 bp upstream of the transcriptional start site. Our data also demonstrate that alterations in SERCA2 expression under inflammatory and hyperglycemic conditions are closely linked with activation of the serine/threonine kinase, cyclin-dependent kinase 5 (CDK5), and posttranslational modification of PPAR-γ, findings that can be reversed either through pharmacologic inhibition of CDK5 or pharmacological activation of PPAR-γ.

Results

SERCA2 expression is down-regulated in models of T2DM

Previously, we have shown that advanced diabetes is associated with profound changes in β-cell Ca^{2+} homeostasis and insulin-secretory function. These changes correlated with altered expression of SERCA2a, SERCA2b, and SERCA3 mRNA expression within the pancreatic islet (26). To study the mechanisms underlying this observation, we first sought to determine the most prevalent SERCA isoform within the pancreatic islet. Using equally efficient primers (Fig. 1A), quantitative RT-PCR (qRT-PCR) was performed using RNA isolated from C57BL6/J mouse islets, and results show that SERCA2b was the most prevalent mRNA species. The expression of the next most abundant isoform, SERCA3, was about 50% of the level observed for SERCA2b. SERCA2a was expressed at extremely low levels (Fig. 1B). *SERCA1* gene expression was not detected (data not shown).

Given these results, the remainder of our studies focused on the SERCA2b isoform. To characterize changes in SERCA2b mRNA and protein expression patterns in rodent models of T2DM, RNA was first isolated from 9-wk-old C57BLKS/J-db/db mice (hereafter referred to as db/db mice), and SERCA2b mRNA expression was com-

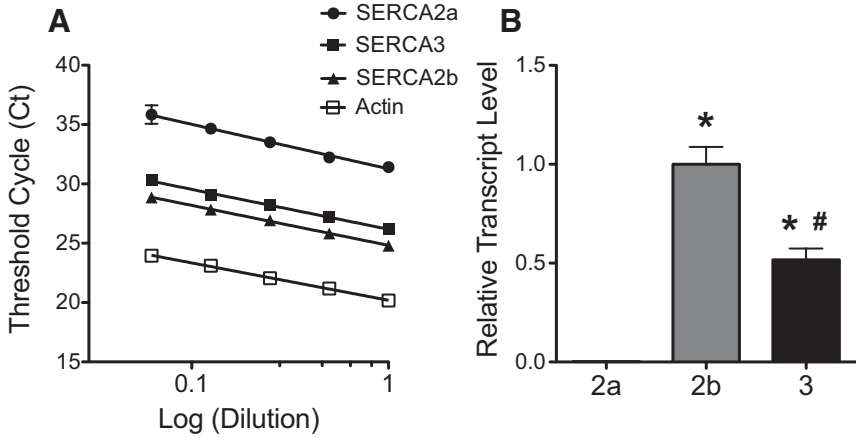

FIG. 1. SERCA2b is the most prevalent isoform expressed in the mouse islet. RNA was isolated from 8-wk-old C57BL6/J mice. A, Quantitative real-time PCR threshold cycles demonstrating linearity of amplification for primer sets from serial 10-fold dilutions of mouse islet reversed-transcribed RNA. B, Reverse-transcribed RNA was subjected to qRT-PCR quantitation of SERCA2a, SERCA2b, and SERCA3 transcript levels using equally efficient primers from panel A. *, Significantly different ($P < 0.05$) compared with SERCA2a transcript levels. #, Significantly different ($P < 0.05$) compared with SERCA2b transcript levels. n = 3 samples for each experiment, and results are displayed as the means ± SEM.

pared with levels observed in islets isolated from lean normoglycemic C57BLKS/J controls. SERCA2b expression levels were significantly lower in db/db mice compared with those observed in the background strain. (Fig. 2A).

Immunoblot was next performed, and SERCA2 protein expression was similarly decreased in islets from diabetic 20 wk-old db/db mice compared with normoglycemic db/+ littermate controls (Fig. 2B). It should be noted that the antibody used did not distinguish between SERCA2 isoforms. Consequently, when referring to the measurement of protein, the term SERCA2 is used preferentially. Blood glucose levels were significantly higher in db/db mice compared with both the C57BLKS/J and db/+ mice, suggesting that islet SERCA2b expression patterns are inversely correlative with glucose homeostasis and directly correlative with diabetes severity (Fig. 2C).

To ensure that this observation was not limited to models with impairments in leptin signaling, we treated C57BL6/J mice with multiple low doses of the DNA alkylating agent streptozotocin (STZ). STZ administered in this manner reliably results in hyperglycemia and inflammatory insulitis (29). Islets were isolated from STZ- and saline-treated mice, and islet SERCA2b mRNA levels were measured by qRT-PCR. Mice treated with STZ were hyperglycemic compared with controls and showed significantly lower levels of SERCA2b mRNA (Fig. 2, D and E). To confirm our findings in human T2DM, RNA was isolated from cadaveric donor islets. SERCA2b mRNA levels were decreased in islets isolated from T2DM donors compared with islets isolated from nondiabetic controls (Fig. 2F).

SERCA2b expression is increased by pioglitazone

In our previous study, daily oral treatment of db/db mice with the PPAR-γ agonist, pioglitazone, for 6 wk markedly improved islet SERCA2b mRNA expression (26). We therefore reasoned the *SERCA2* gene might be a direct transcriptional target of the nuclear receptor PPAR-γ. To test this hypothesis, we first incubated INS-1 cells and mouse and human and islets with 10 μM pioglitazone for 24 h. In all three model systems, incubation with pioglitazone significantly increased expression of SERCA2b mRNA (Fig. 3, A–C). Immunofluorescence was performed on pancreatic sections from 14-wk-old C57BLKS/J and db/db mice that had been treated either with saline or pioglitazone by daily oral gavage for 6 wk as described previously (26). Results show diminished SERCA2 protein expression in db/db mice compared with normoglycemic controls. Systemic pioglitazone treatment restored SERCA2 staining intensity (Fig. 3D).

PPAR-γ is a direct transcriptional regulator of the *SERCA2* gene

To determine whether the observed transcriptional effects were direct, we then scanned the human *SERCA2* promoter for PPREs. We identified five putative PPRE-like elements. Although none had direct homology to previously published PPRE sequences, several similarities with known PPREs were noted (30–36) (Fig. 4A). We next performed reporter gene assays using fragments of the human *SERCA2* promoter as depicted in Fig. 4B. Constructs were transfected into INS-1 cells, which were then treated with 10 μM pioglitazone for 72 h. Pioglitazone treatment increased luciferase expression nearly 1.5- to 3-fold in all of the constructs tested. Both basal and pioglitazone-stimulated luciferase expression was blocked by deletion of the region of the promoter between −259 and −25 bp upstream of the transcriptional start site (Fig. 4B), suggesting that the PPRE closest to the transcriptional start site might serve as the key regulatory region for PPAR-γ-mediated transcriptional regulation of the *SERCA2* gene. Figure 4C shows the close homology of this PPRE between several species including human, mouse, rat, and rabbit. The PPAR-γ and retinoid X receptor binding sequences are noted in Fig. 4C. The variant base among species occupies

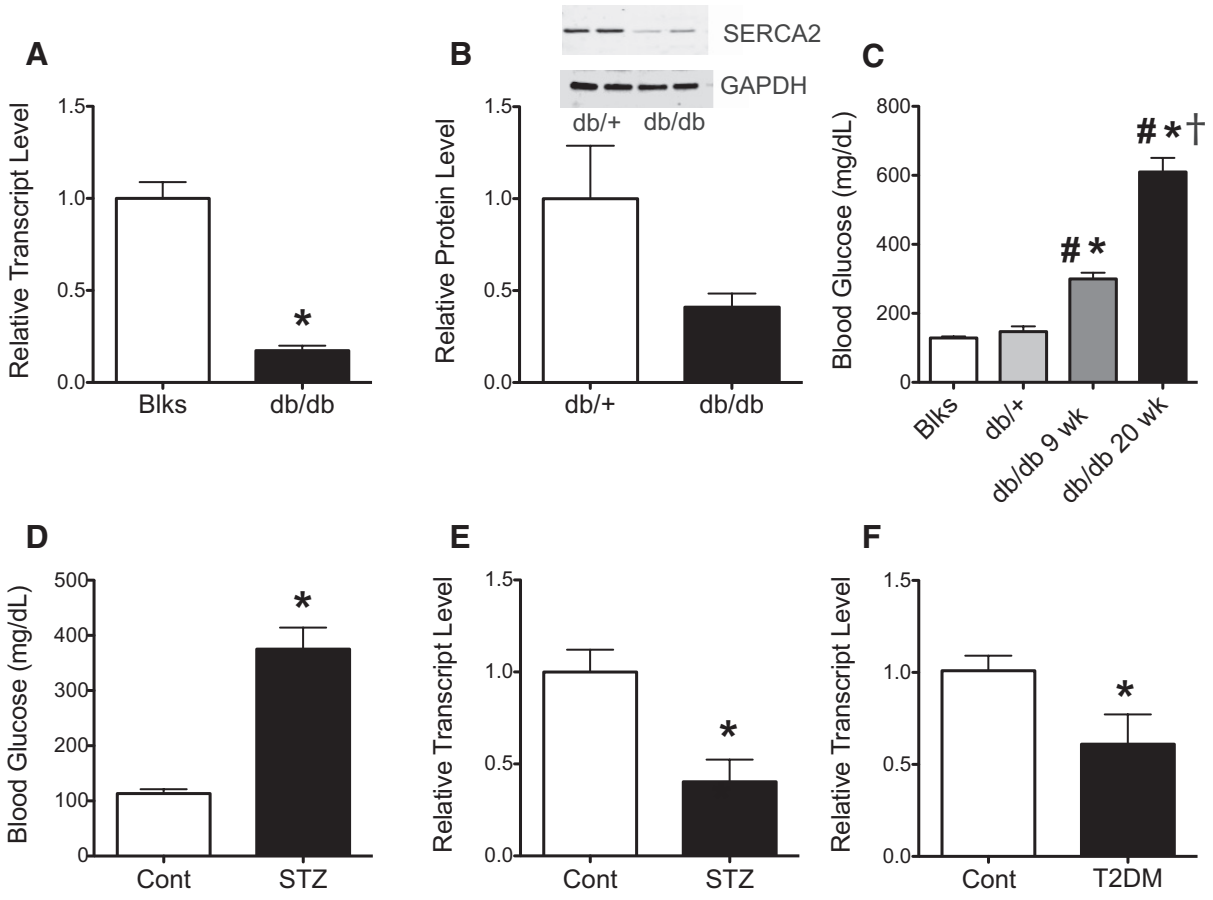

FIG. 2. Islet SERCA2b mRNA and SERCA2 protein levels are decreased in murine and human models of diabetes. A, RNA was isolated from 9-wk-old male C57BLKS/J (Blks) and C57BLKS/J-db/db (db/db) mouse islets. Reverse-transcribed RNA was subjected to real-time PCR for quantitation of SERCA2b transcript levels. *, Significantly different ($P < 0.05$) compared with C57BLKS/J mice. B, Protein was isolated from 20-wk-old C57BLKS/J-db/+ (db+) and C57BLKS/J-db/db mouse islets. Immunoblotting was performed using antibodies against SERCA2 and glyceraldehde-3-phosphate dehydrogenase (GAPDH). C, Random blood glucose values at the time of experiment termination. *, Significantly different ($P < 0.05$) compared with Blks mice. #, Significantly different ($P < 0.05$) compared with db/+ mice. †, Significantly different ($P < 0.05$) compared with 9-wk-old db/db mice. D and E, Male 8-wk-old C57BL6/J mice were treated with either saline (Cont) or STZ at a dose of 55 mg/kg/d daily for 5 d. D. Random blood glucose levels 4 wk after STZ treatment. *, Significantly different ($P < 0.05$) compared with saline-treated mice. E, RNA was isolated from mouse islets, reverse transcribed, and subjected to qRT-PCR quantitation of SERCA2b transcript levels. *, Significantly different ($P < 0.05$) compared with saline-treated mice. F, Relative transcript level of SERCA2b in cadaveric islets from normoglycemic (Control) and T2DM donors. Significantly different ($P < 0.05$) compared with SERCA2b mRNA levels in normoglycemic islets. n = at least 3 samples for each experiment with the exception of panel B, in which n = 2 samples of 100 islets from three biological replicates, and results are displayed as the means ± SEM.

the spacing position of this direct repeat 1 PPRE, which contains a typical 6-N-6 configuration.

As confirmation of our findings, luciferase assays were performed following site-directed mutagenesis of the −259 bp construct. Three bases pairs in the proximal PPRE were changed according to the *schematic* shown in Fig. 4D. Results showed a significant decrease in both basal and pioglitazone-stimulated luciferase expression. Furthermore, transfection of a dominant-negative PPAR-γ expression construct was able to block luciferase expression under basal and pioglitazone-stimulated conditions (Fig. 4E).

EMSA were next performed using INS-1 cell nuclear extract and a probe containing the −55 to −24 fragment of the human *SERCA2* promoter. The addition of nuclear extract in Fig. 5A demonstrates that PPAR-γ does, in fact, bind this region of the human *SERCA2* promoter (lane 2). Loss of the shifted complex is observed after competition assays, which were performed by adding excess nonlabeled probe to the reaction mixture (lane 3). Furthermore, mutation of the PPRE in the cold probe prevented the loss of this complex (lane 4). The shifted complex (indicated by the *arrow*) contained two bands with a more prominent lower band. The competition assay resulted in loss of the prominent lower band with some decrease in the upper band as well, suggesting that PPAR-γ binds as part of a complex that may include other cofactors.

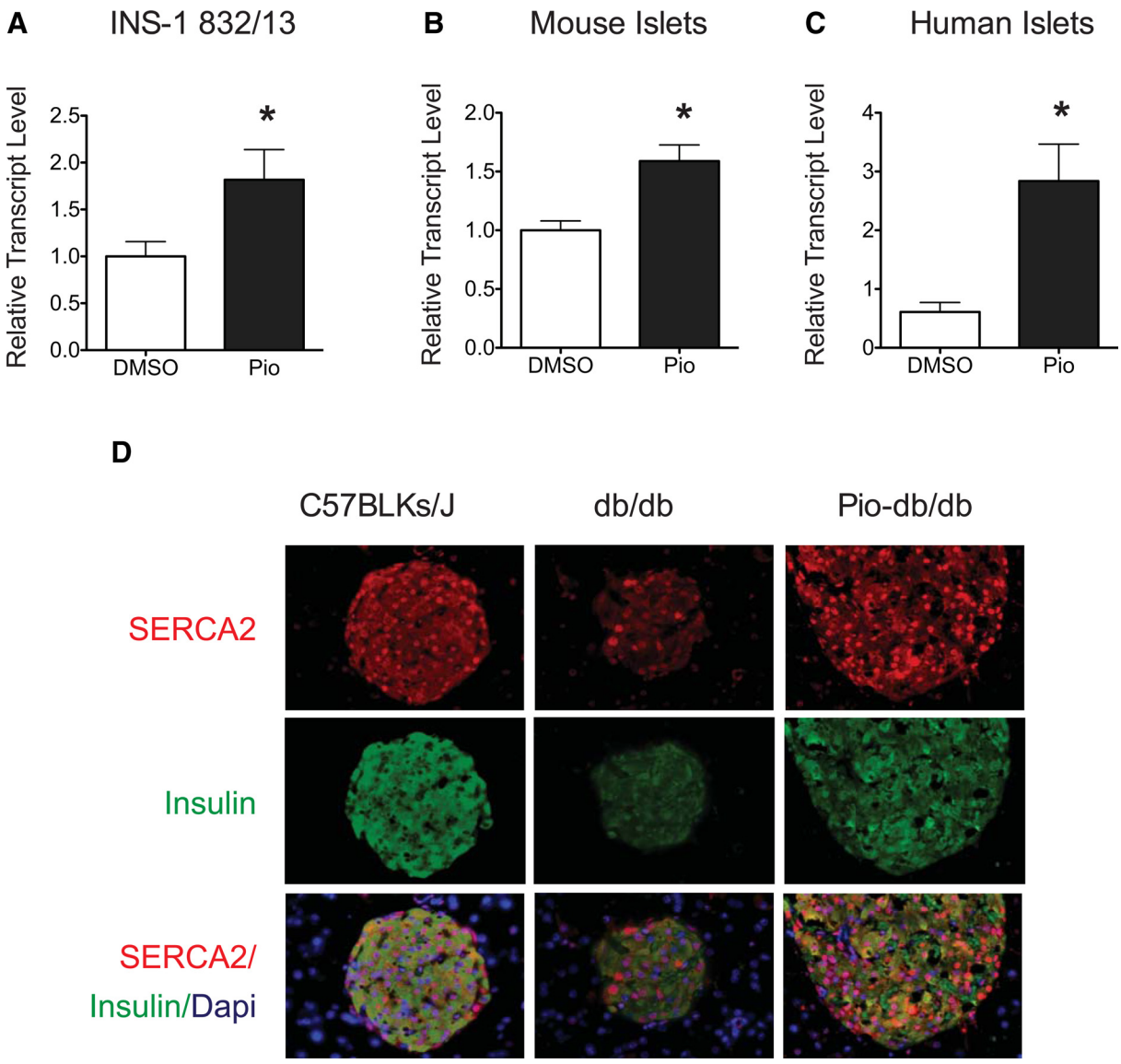

FIG. 3. Pioglitazone (Pio) increases SERCA2b mRNA and protein expression. RNA was isolated from INS-1 832/13 cells (A), 8-wk-old C57BL6/J mouse islets (B), and cadaveric human islets from a donor with T2DM (C) were cultured with 10 μM pioglitazone (Pio) or dimethylsulfoxide (DMSO) for 24 h. Reverse-transcribed RNA was subjected to real-time RT-PCR to quantitate SERCA2b transcript levels. *, Significantly different ($P < 0.05$) compared with DMSO-treated control samples. n = 3 samples for each experiment, and results are displayed as the means ± SEM. D, Pancreata from male db/db mice treated with vehicle (db/db) or pioglitazone (Pio-db/db) by daily oral gavage for 6 wk were fixed, stained, and compared with age- and sex-matched lean C57BLKS/J pancreata. Dapi, 4′,6-Diamidino-2-phenylindole.

For *in vivo* confirmation, chromatin immunoprecipitation (ChIP) experiments were performed using whole-cell extract isolated from INS-1 cells. Results showed a 4-fold increase in recovery of the proximal *SERCA2* promoter after immunoprecipitation with anti-PPAR-γ antibody compared with immunoprecipitation with normal rabbit serum (Fig. 5B). As a second negative control, PCR was performed to amplify *β-actin* genomic DNA, and percent recovery of the *β-actin* promoter was similar to results obtained with normal rabbit serum. Taken together, results from the luciferase, EMSA, and ChIP experiments suggest that PPAR-γ is a direct transcriptional regulator of the *SERCA2* gene.

Loss of SERCA2 results in alterations in β-cell calcium homeostasis, secretory function, and survival, parameters that are partially restored by PPAR-γ activation

To recapitulate our *in vivo* findings and study further the functional relevance of SERCA2b down-regulation in the pancreatic β-cell, we next sought to create a cell-based system that would mimic the metabolic milieu of T2DM. Given an evolving appreciation of both systemic and locally derived cytokines and activation of the innate immune system in the pathogenesis of T2DM (37–41), INS-1 832/13 cells were treated with 5 ng/ml of the proinflammatory cytokine IL-1β and 25 mM glucose (1L-

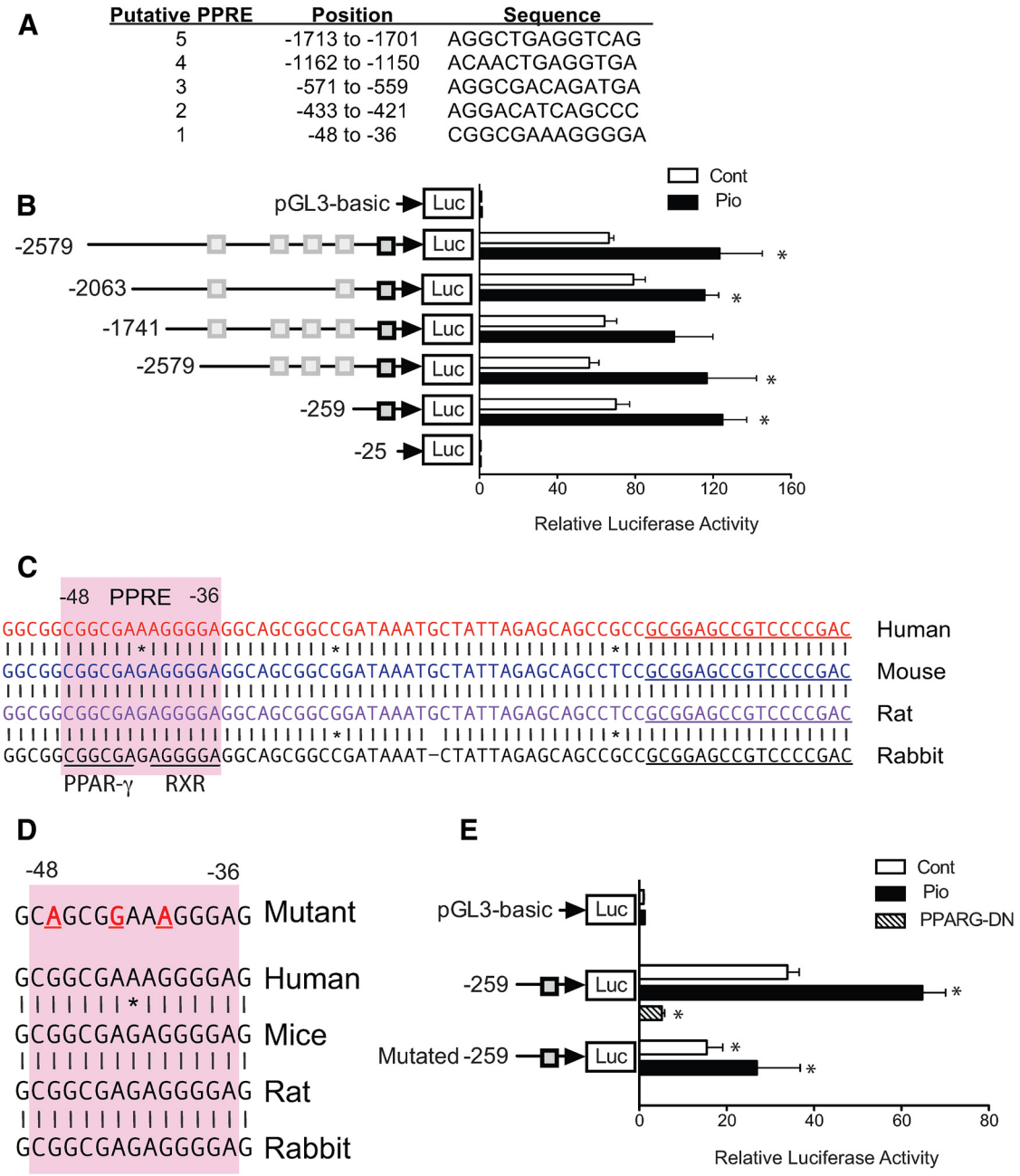

FIG. 4. Localization of the PPRE in the human *SERCA2* promoter. A, Five putative PPREs were identified in the human *SERCA2* promoter. B, Deletion constructs were generated and transfected into INS-1 cells, which were cultured in the presence or absence of pioglitazone (Pio) or DMSO (Cont) for 72 h. C, Schematic showing sequence of proximal putative PPAR-γ binding site in the −259-bp construct and conservation among species. The PPAR-γ- and retinoid X receptor-binding sites within the PPRE are denoted and indicate that the variant base among species occupies the spacing position of this direct repeat 1. D, Schematic illustrating site-directed mutagenesis strategy. E, Mutation analysis of putative binding site in the −259-bp *SERCA2* promoter construct. Wild-type and mutated constructs were transfected into INS-1 cells and cultured in the presence or absence of pioglitazone or DMSO control. Wild-type constructs were also cotransfected with PPAR-γ dominant negative construct (PPARG-DN). In all cases, cells were harvested after a 72-h treatment, and reporter activity was measured and normalized to total protein content. Results are the means ± SEM for three independent experiments performed in triplicate. *, Significantly different ($P < 0.05$) compared with DMSO (Cont) treatment in wild-type construct.

1β+high glucose [HG]) for 6 and 24 h. We observed a progressive decline in SERCA2b mRNA levels over time (Fig. 6A). Similar to our *in vivo* observations (26), pioglitazone was able to restore SERCA2b mRNA levels under diabetic conditions (Fig. 6B). Treatment with IL-1β and high glucose resulted in decreased insulin release after glucose stimulation. This effect was partially restored with pioglitazone treatment (Fig. 6C). Consistent with a decrease in SERCA2 expression and activity, IL-1β and high glucose resulted in increased basal cytosolic calcium

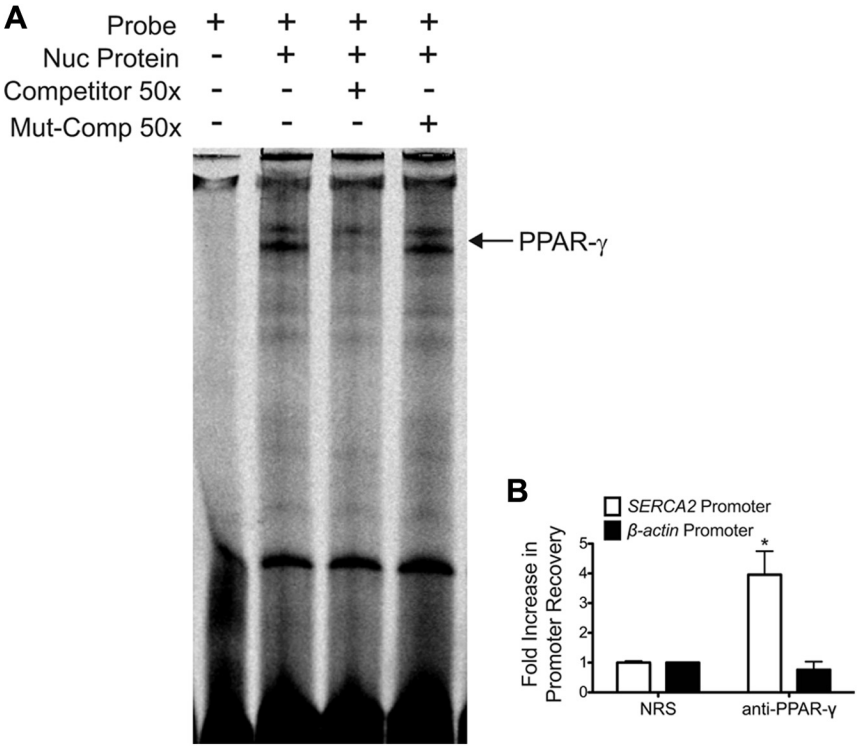

FIG. 5. PPAR-γ binds to a proximal PPRE in the human *SERCA2* promoter. A, INS-1 cell nuclear extract (1 μg) was used in gel shift mobility assays using either IRDye-labeled or unlabeled oligonucleotides spanning the −55- to −24-bp fragment of the human *SERCA2* promoter. Excess unlabeled probe (Competitor 50X) was added in lane 3, whereas unlabeled mutated probe (Mut-Comp 50X) was added in excess in lane 4. DNA-protein complexes were resolved by electrophoresis as described in *Materials and Methods*. Data shown are representative of three independent experiments. B, INS-1 cells were harvested and subjected to ChIP analysis as detailed in *Materials and Methods*. Quantitative PCR was used to measure recovery of the proximal *SERCA2* promoter after immunoprecipitation with anti-PPAR-γ antibody or normal rabbit serum (NRS). PCR amplification of *β-actin* genomic DNA was performed as an additional negative control. Results are expressed as fold increase in percent recovery of the target gene compared with NRS, and represent the means ± SEM for three independent experiments. *, Percent recovery of the *SERCA2* gene after immunoprecipitation with anti-PPAR-γ antibody was statistically different ($P < 0.05$) compared with immunoprecipitation with NRS.

levels. Again in the context of high glucose and cytokine stress, pioglitazone was able to partially rescue basal cytosolic calcium levels in both INS-1 cells (Fig. 6D) and human islets (Fig. 6E) treated with IL-1β and 25 mM glucose. Treatment with IL-1β and 25 mM glucose led to increased cell death as assessed by activation of caspase-3, a finding that was significantly decreased by pioglitazone (Fig. 6F).

SERCA2b overexpression partially protects against cytokine- and high glucose-induced secretory dysfunction

To directly show that the effects of pioglitazone on insulin secretion were mediated through alterations in SERCA2b expression levels, INS-1 cells were transfected with a human flag-tagged SERCA2b expression construct and treated accordingly with IL-1β + HG. Figure 7A confirms that SERCA2b was overexpressed in our *in vitro* system. As indicated in Fig. 7B, under conditions of high glucose and cytokine stress with IL-1β, SERCA2b overexpression was able to also partially restore insulin secretion. The magnitude of this rescue was similar to results obtained with pioglitazone. Interestingly, overexpression of SERCA2b under basal conditions also led to a significant increase in GSIS.

CDK5 activation disturbs SERCA2 protein expression through Ser-273 phosphorylation of PPAR-γ

We next sought to understand the mechanisms underlying the observed loss of SERCA2b expression in the diabetic β-cell. A recent article by Choi *et al.* (42) suggests that serine-273 phosphorylation of PPAR-γ by activated CDK5 under inflammatory conditions leads to a loss of PPAR-γ transcriptional activity in adipocytes. To test this pathway in the β-cell, INS-1 cells were treated with IL-1β and 25 mM glucose in time course experiments. The results are shown in Fig. 8A. Within 2 h, tyrosine-15 phosphorylation of CDK5, a modification associated with activation of the kinase (43), was observed. Similarly, increased ser-273 phosphorylation of PPAR-γ was noted at 2 h, with no significant changes in total PPAR-γ levels. These changes preceded translation of significant levels of inducible nitric oxide synthase protein in response to cytokine signaling. In the context of CDK5 activation and phosphorylation of PPAR-γ, SERCA2 protein levels also began to decrease within 2 h and decreased further in a time-dependent manner. Increased tyrosine-15 phosphorylation of CDK5 was noted through 24 h of high glucose and cytokine treatment, but levels decreased by 48 h, corresponding to a decrease in total CDK5 levels (Fig. 8A). Activation of CDK5 requires association of a regulatory protein and depending on the context this regulatory protein can be either p35, p39, or p25 (44). We next measured expression of CDK5's usual binding partner, p35; however, no change in p35 expression levels was observed in INS-1 cells treated with high glucose and IL-1β.

Interestingly, pharmacological inhibition of CDK5 with roscovitine was able to prevent down-regulation of

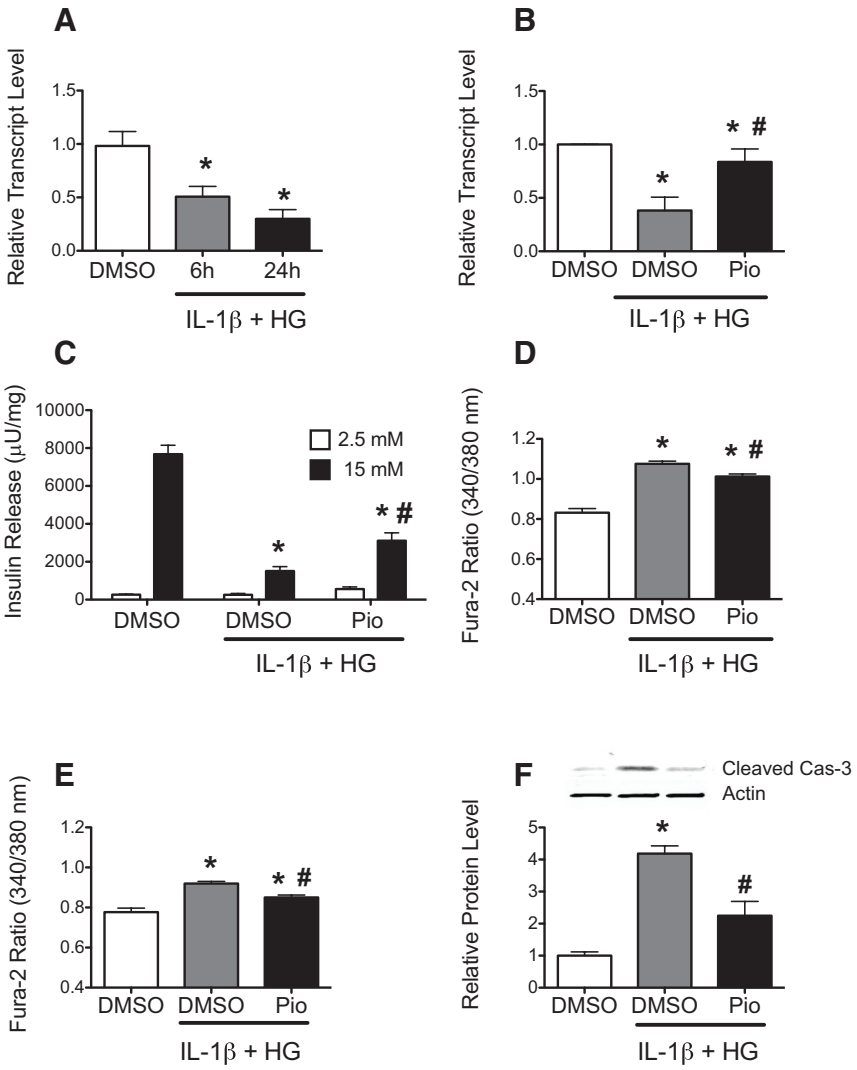

FIG. 6. PPAR-γ activation rescues SERCA2 expression and improves insulin-secretory function in an *in vitro* model of diabetes. A, RNA was isolated from INS-1 cells treated with IL-1β and 25 mM glucose (IL-1β + HG) for 6 and 24 h, and qRT-PCR was performed to measure SERCA2b mRNA levels. B, INS-1 cells were treated with IL-1β + HG for 6 h after pretreatment with pioglitazone (Pio) for 16 h. B, SERCA2b mRNA levels were measured by qRT-PCR. C, GSIS was measured as described in *Materials and Methods* after incubation in 2.5 mM and 15 mM glucose. D, The fura-2AM fluorescence ratio was measured as described in *Materials and Methods* in INS-1 cells. E, Cadaveric human islets from a nondiabetic donor were treated with IL-1β + HG in the presence or absence of pioglitazone, and the fura-2AM fluorescence ratio was measured. F, Total protein was isolated from INS-1 cells treated with IL-1β + HG in the presence or absence of pioglitazone and subjected to immunoblot analysis for cleaved-caspase 3 (Cas-3). B, Quantitative protein levels are shown graphically. *, Statistically significant ($P < 0.05$) compared with DMSO control. #, Statistically significant ($P < 0.05$) compared with IL-1β + HG treatment without pioglitazone. Results are displayed as the means ± SEM, where n = at least three independent experiments.

SERCA2 protein levels and inhibit phosphorylation of PPAR-γ. The same effects were seen with pioglitazone treatment (Fig. 8, A and B). Taken together, these results suggest that CDK5 activation in response to high glucose and inflammatory cytokines in the β-cell leads to Ser-273 phosphorylation of PPAR-γ and loss of SERCA2 expression.

In support of this model, protein was isolated from cadaveric human islets from normoglycemic and T2DM donors. Islets from diabetic donors showed decreased total SERCA2 expression as well as increased CDK5 activation and increased levels of Ser-273 phosphorylated PPAR-γ. Interestingly, and in contrast to INS-1 cells, increased expression of p35 was observed in diabetic human islets (Fig. 9).

Discussion

The divalent cation, Ca^{2+}, plays an important role in several aspects of normal β-cell health. In particular, the maintenance of a robust pool of Ca^{2+} in the ER plays a key role in several aspects of β-cell function including insulin production and secretion and the maintenance of ER health (8, 12, 21, 25). The SERCA pump resides in the ER membrane and hydrolyzes one ATP molecule to move two Ca^{2+} molecules across the sarco- or ER membrane. The major goal of our study was to define functional consequences and underlying mechanisms of β-cell SERCA2b dysregulation in the context of T2DM.

Here, we have identified SERCA2b as the predominant SERCA isoform expressed in the pancreatic islet. Transcriptional profiling revealed that SERCA2b is expressed at about twice the level of SERCA3, whereas SERCA2a was expressed at very low levels within the pancreatic islet. We detected no expression of SERCA1. SERCA2a is expressed in the sarcoplasmic reticulum of the heart, slow-twitch skeletal muscle, and smooth muscle, whereas SERCA2b is ubiquitously expressed. SERCA3 is found in a variety of tissues; however, its expression is more limited compared with 2b (24). Although a number of different SERCA isoforms have been identified, structural analysis and developmental studies suggest distinct roles for many of these isoforms. Of the 11 isoforms, SERCA2b has the highest calcium affinity and therefore the lowest catalytic turnover, functional properties that have been recently explained in an elegant structural analysis of the SERCA2b molecule (45). SERCA2b contains a C-terminal extension of 49 residues called the 2b-tail. This region provides an elev-

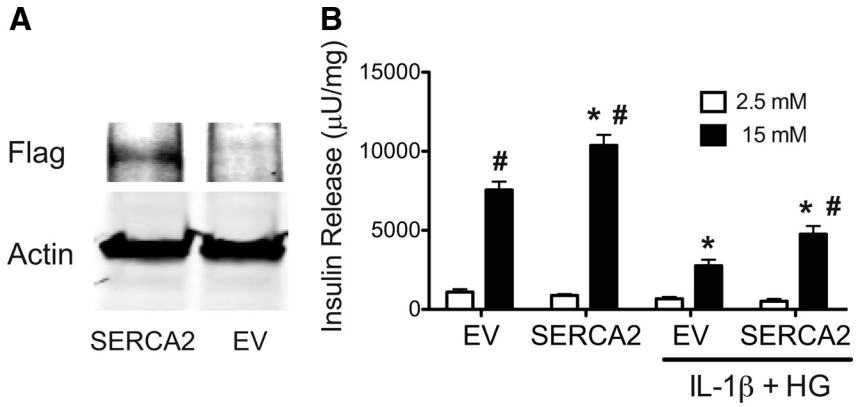

FIG. 7. SERCA2 overexpression rescues insulin-secretory function after high glucose and cytokine treatment. INS-1 cells were transfected with empty vector (EV) or a human SERCA2 expression vector containing a C-terminal Myc-DDK (Flag) tag. A, Total protein was isolated from transfected cells, and immunoblot for Flag was performed. Actin was used as a loading control. B, Transfected INS-1 cells were treated with DMSO or IL-1β + 25 mM glucose for 6 h. GSIS was measured. *, Statistically different ($P < 0.05$) compared with EV without IL-1β + HG. #, Statistically different compared with EV with IL-1β + HG. Results displayed as the means ± SEM, where n = at least three independent experiments.

enth transmembrane domain and luminal extension that is unique to SERCA2b. Vandecaetsbeek *et al.* (45) have shown that direct interaction of this region with upstream luminal loops of the protein leads to stabilization of the Ca^{2+}-bound isoform, thereby explaining the increased calcium affinity of SERCA2b. In support of distinct roles for SERCA isoforms in the β-cell, a previous analysis of total body SERCA3 knockout mice indicated that SERCA3 ablation was insufficient to impair glucose homeostasis or insulin secretion. Deficiency of SERCA3 did not lead to increased basal cytosolic Ca^{2+} levels (46, 47), as was observed in the present study as well as our previous analysis of Ca^{2+} homeostasis in db/db islets (26). Interestingly, loss of SERCA3 is associated with alterations in cytosolic Ca^{2+} oscillations (46). Similarly, in db/db islets, in which both SERCA2b and SERCA3 are down-regulated, marked diminution in oscillations were also observed (26). Under both normal and stressed conditions in our study, transient overexpression of SERCA2b significantly increased insulin secretion. These results suggest that in contrast to SERCA3, SERCA2b likely plays a larger role in regulated insulin secretion.

We and others have shown that SERCA2b is down-regulated in the rodent diabetic islet (26–28). Here we show that SERCA2b expression is also significantly decreased in human islets isolated from cadaveric T2DM diabetic donors. *In vitro* experiments demonstrate that SERCA2b is specifically down-regulated in the presence of high glucose (25 mM) and inflammatory cytokines. Numerous clinical and preclinical studies clearly demonstrate that thiazolidinediones, which act as agonists of PPAR-γ, have direct effects to improve pancreatic β-cell function and survival in T2DM (11). Our data indicate that SERCA2b is directly regulated by the orphan nuclear receptor PPAR-γ. Further, we identify what we believe is a novel PPRE (CGGCGA A AGGGGA) in the proximal human SERCA2 promoter that has high similarity to rat, mouse, and rabbit promoter sequences (Fig. 4D).

Although we hypothesize a direct effect on the *SERCA2* promoter, our data do not exclude the possibility that PPAR-γ might also modulate maladaptive chromatin architecture responsible for *SERCA2* transcriptional down-regulation in diabetes. In fact, an integrated computational genomics approach was recently used to produce a genome-wide library of high confidence PPAR target genes. Results from this analysis predict that PPAR-γ might regulate a number of chromatin-modifying genes (34). In support of this, our previous work has shown that systemic treatment of db/db mice with pioglitazone improved euchromatin architecture at key β-cell loci including the *insulin* and *GLUT2* promoters (26). Although we have identified this most proximal element to be a functional PPRE, one limitation of our study is that the design of our reporter constructs does not allow us to detect cooperativity between the five putative PPREs.

In addition to this direct transcriptional effect, we also show that pioglitazone preserves SERCA2b expression through modulation of CDK5 activity and PPAR-γ phosphorylation. Recently, Choi *et al.* (42) showed in adipocytes that CDK5 phosphorylated PPAR-γ at the serine-273 residue, leading to transcriptional inefficiency of the nuclear receptor. PPAR-γ phosphorylation was increased after high-fat diet feeding and reversed by small interfering RNA-mediated and pharmacological inhibition of CDK5. Interestingly in this study, rosiglitazone, a CDK5 inhibitor, was also able to block serine-273 phosphorylation of PPAR-γ and restore transcription of key target genes like adiponectin. To explain this finding, hydrogen/deuterium exchange mass spectrometry was performed and showed that ligand binding led to a conformational change in PPAR-γ, which prevented CDK5-mediated Ser-273 phosphorylation (42).

To determine whether a similar paradigm could be applied in the β-cell, we measured Ser-273 phosphorylation of PPAR-γ and activation of CDK5 in INS-1 cells after exposure to high glucose and cytokine stress. Interestingly, we observed a reciprocal relationship between PPAR-γ phosphorylation and SERCA2 expression. Both PPAR-γ phosphorylation and SERCA2 loss were blocked

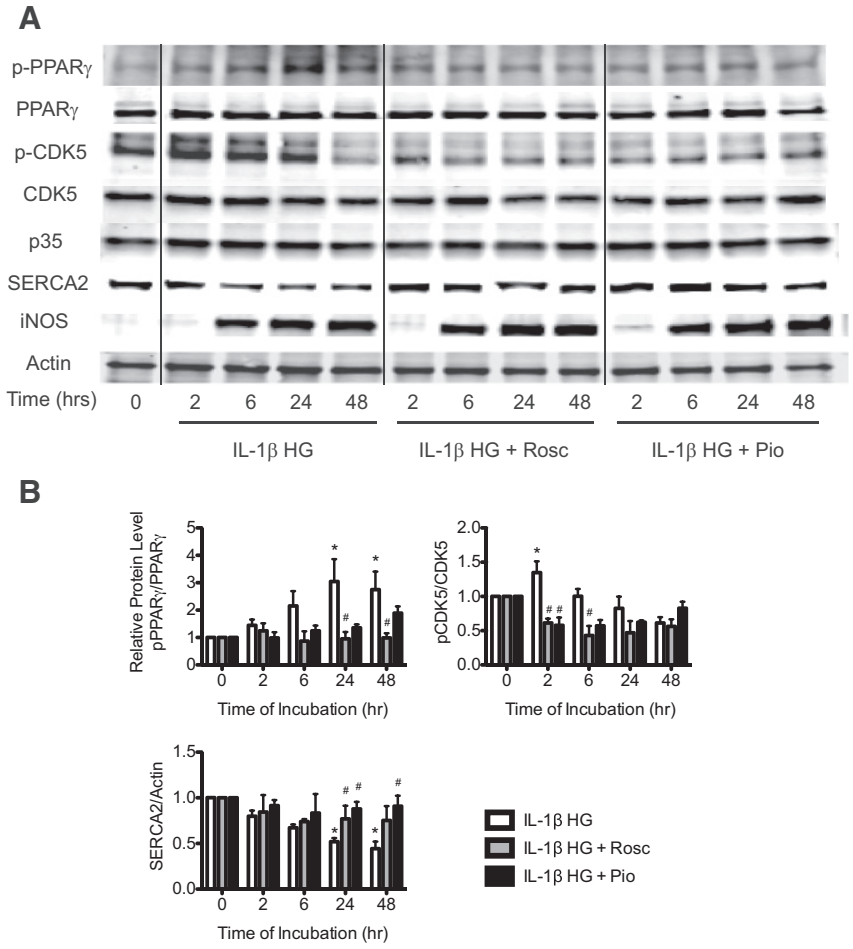

FIG. 8. SERCA2 down-regulation is prevented by inhibition of CDK5 and PPAR-γ phosphorylation. A, INS-1 cells were treated with IL-1β and 25 mM glucose (IL-1β HG) for 2, 6, 24, and 48 h combined with either DMSO, 10 μM roscovitine (Rosc), or 10 μM pioglitazone (Pio). Total protein was isolated and immunoblotting was performed for serine-273-phosphorylated PPAR-γ (p-PPARγ), total PPAR-γ, tyrosine-15-phosphorylated CDK5 (p-CDK5), total CDK5, p35, SERCA2, and inducible NOS (iNOS). Actin was used a loading control. B, Quantitative protein levels are shown graphically. *, Statistically different ($P < 0.05$) compared with time zero (no treatment). #, Statistically different ($P < 0.05$) compared with IL-1β + HG alone. Results are representative of three independent experiments.

by pharmacological inhibition of CDK5 with roscovitine or treatment with the PPAR-γ agonist pioglitazone. Although loss of SERCA2 correlated strongly with activation of CDK5, one potential weakness of our data is that roscovitine in not a specific CDK5 inhibitor and has activity against other cyclin-dependent kinases (48).

Although our data would suggest a maladaptive role for CDK5 in the β-cell under hyperglycemia and cytokine stress, previous literature indicates a mixed role for CDK5 in islet physiology. Genome-wide association studies have identified polymorphisms in CDK5-regulatory subunit-associated protein1-like 1 (CDKAL1) that predispose to T2DM (49–51). CDKAL1 binds to p35 and inhibits CDK5 activity (52).

The function of CDK5 has been best studied in the neuronal system, where it is associated with both pro-survival and pro-apoptotic effects. The role of CDK5 in the regulated insulin-secretory pathway is unclear, with studies showing both positive and negative results (53–57). In the context of glucose toxicity, inhibition of CDK5 with roscovitine prevented hyperglycemia-induced loss of *insulin* and *pdx1* gene expression (58). Of note, the *pdx1* gene is known to be a direct target of PPAR-γ in the β-cell (31). A second study showed that overexpression of p35 in mouse insulinoma cells led to apoptosis (59).

Many of the pro-apoptotic functions of CDK5 occur within the context of hyperactivation of the kinase, which follows cleavage of p35 to p25 by the calcium-activated protease, calpain. Hyperactivation of CDK5 in the central nervous system is linked to the pathophysiology of Alzheimer's disease (44, 60–62). Given similarities between the pathophysiology of Alzheimer's disease and T2DM, Daval *et al.* (63) recently pursued the hypothesis that CDK5 might mediate β-cell death induced by islet-amyloid polypeptide. Surprisingly, they describe a protective role for CDK5 in rat islets that overexpress human islet amyloid polypeptide. They further showed that in a normal, unstressed environment, loss of CDK5 in rat islets and INS-1 cells led to increased apoptosis through loss of focal adhesion kinase activity.

Clearly, the existing literature and our study point to a deep complexity regarding the physiology of CDK5 in the β-cell under both normal and diabetic conditions. We propose the hypothesis that the role of CDK5, as in the neuronal system, is context dependent and may favor either survival or death depending on the conditions studied and whether the regulatory subunit is p39, p35, or p25. Model Fig. 10 provides an overall summary of our experimental findings. Taken together, our data indicate that dysregulation of SERCA2b plays a prominent role in the progressive β-cell death and dysfunction observed in T2DM. Our data also suggest that pharmacological activation of PPAR-γ has dual effects to preserve SERCA2b expression. First, PPAR-γ acts as a direct transcriptional regulator, and pharmacological activation with PPAR-γ ligands is expected to increase gene transcription. In ad-

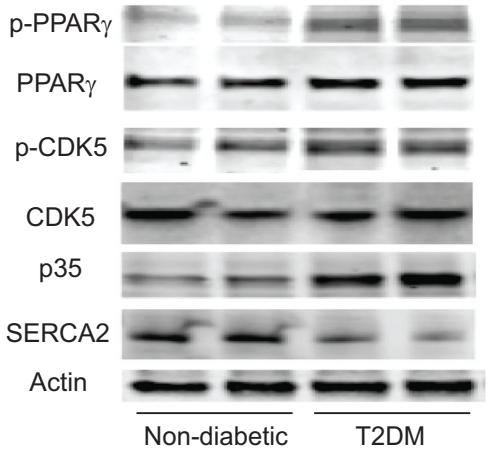

FIG. 9. Loss of SERCA2 expression is observed in human diabetes and occurs within the context of PPAR-γ phosphorylation and CDK5 activation. Total protein was isolated from cadaveric human islets from nondiabetic and T2DM donors. Immunoblot was performed for Ser-273-phosphorylated PPAR-γ, total PPAR-γ, Tyr-15-phosphorylated CDK5, total CDK5, p35, and SERCA2.

dition, treatment with pioglitazone inhibits CDK5-mediated PPAR-γ phosphorylation and prevents transcriptional inefficiency of the nuclear receptor. Restoration of SERCA2b expression, either through targeted pharmacological activation of PPAR-γ or inhibition of CDK5 may be viable therapeutic approaches to improve β-cell function and survival in the context of the hyperglycemic and cytokine stress that typifies T2DM.

Materials and Methods

Cell culture and primary human islet preparations

INS-1 cells (832/13) were cultured in RPMI-1640 containing 11.1 mM glucose supplemented with 10% fetal bovine serum, 100 U/ml penicillin, 100 μg/ml streptomycin, 10 mM HEPES, 2 mM L-glutamine, 1 mM sodium pyruvate, and 50 μM β-mercaptoethanol. Human islets isolated from cadaveric nondiabetic and diabetic donors were obtained from Beta-Pro, LLC, the National Disease Research Interchange, or the Integrated Islet Distribution Program. On arrival, islets were immediately placed in DMEM containing 5.5 mM glucose, 10% fetal bovine serum, 100 U/ml penicillin, and 100 μg/ml streptomycin (Invitrogen, Carlsbad, CA) and incubated overnight at 37 C with 5% CO_2. Our analysis included islets from seven nondiabetic donors and six donors with T2DM. The average age of nondiabetic donors was 48.9 ± 6 yr (SEM). The average body mass index (BMI) was 25.1 ± 1.8 kg/m^2. The mean age of diabetic donors was 52.4 ± 4 yr, and the average BMI was 33.1 ± 1.6 kg/m^2. There was no statistical difference in age ($P = 0.38$) or BMI ($P = 0.63$) between the two groups.

Animals and islet isolation

Male C57BL6/J mice were obtained from The Jackson Laboratory (Bar Harbor, ME) at 8 wk of age. Selected mice were treated with ip streptozotocin to induce hyperglycemia at a dose of 55 mg/kg/d for 5 consecutive days. Male C57BLKS/J, C57BLKS/J-db/db mice, and littermate heterozygous controls (db/+) were obtained from The Jackson Laboratory at 8 wk of age and either allowed to age or treated with daily oral gavage of saline or pioglitazone (Takeda Pharmaceuticals, Deerfield, IL) at a dose of 20 mg/kg/d for 6 wk as previously described (26). Animals were maintained under protocols approved by the Indiana University School of Medicine Institutional Animal Care and Use Committee using Association for Assessment and Accreditation of Laboratory Animal Care guidelines. Mice were kept in a standard light-dark cycle with regular access to a chow diet and water *ad libitum*. At the time of euthanasia, blood was sampled from the tail and blood glucose concentrations were determined using an AlphaTRAK glucometer (Abbott Laboratories, Abbott Park, IL). At designated time points, pancreatic islets were isolated by collagenase digestion as described previously (64). Isolated islets were hand picked and cultured in phenol-red free low-glucose DMEM overnight before use. For *in vitro* incubations with pioglitazone, islets were allowed to recover overnight and then incubated with pioglitazone dissolved in 0.1% dimethylsulfoxide (DMSO) to achieve a final concentration of 10 μM.

Quantitative RT-PCR (qRT-PCR)

INS-1 cells (832/13) and islets were washed and processed for total RNA using Qiagen's RNeasy kit (QIAGEN, Valencia, CA), according to the manufacturer's instructions. For qRT-PCR experiments, total RNA (5 μg) was reverse-transcribed at 37 C for 1 h using 15 μg random hexamers, 0.5 mM deoxynucleotide triphosphate, 5× first-strand buffer, 0.01 mM dithiothreitol, and 200 U of Moloney murine leukemia virus reverse transcriptase (Invitrogen) in a final reaction volume of 20 μl. qRT-PCR was performed as described previously (65). Relative RNA levels were established against the invariant β-actin mRNA species, using the comparative C_T method, as described previously (66). Primer sequences are provided in Supplemental Table 1 published on The Endocrine Society's Journals Online web site at http://mend.endojournals.org.

Immunoblot analysis

Supplemental Table 2 contains a complete list of the antibodies and antibody dilutions used in this report. For immunoblot analysis, approximately 1.5 × 10^5 INS-1 cells or 100–125 human or mouse islets were preincubated in RPMI 1640 medium with 2.5 mM glucose for 24 h in the presence or absence of 10 μM pioglitazone or 10 μM roscovitine and then treated with or without a combination of 5 ng/μl of IL-1β and 25 mM glucose for designated time points. Total protein (20 μg) was separated by SDS-PAGE, transferred to a polyvinylidene fluoride membrane, and incubated at 4 C overnight with primary antibodies as summarized in Supplemental Table 2. Bound primary antibodies were detected with antimouse donkey antibody (1:10,000 dilution), antigoat donkey antibody (1:10,000 dilution), or antirabbit donkey antibody (1:10,000 dilution). Immunoreactivity was visualized using fluorometric scanning on an Odyssey imaging system (LI-COR Biosciences, Lincoln, NE).

Immunofluorescence

After euthanasia and intracardiac administration of 4% paraformaldehyde, pancreata were rapidly dissected, paraffin

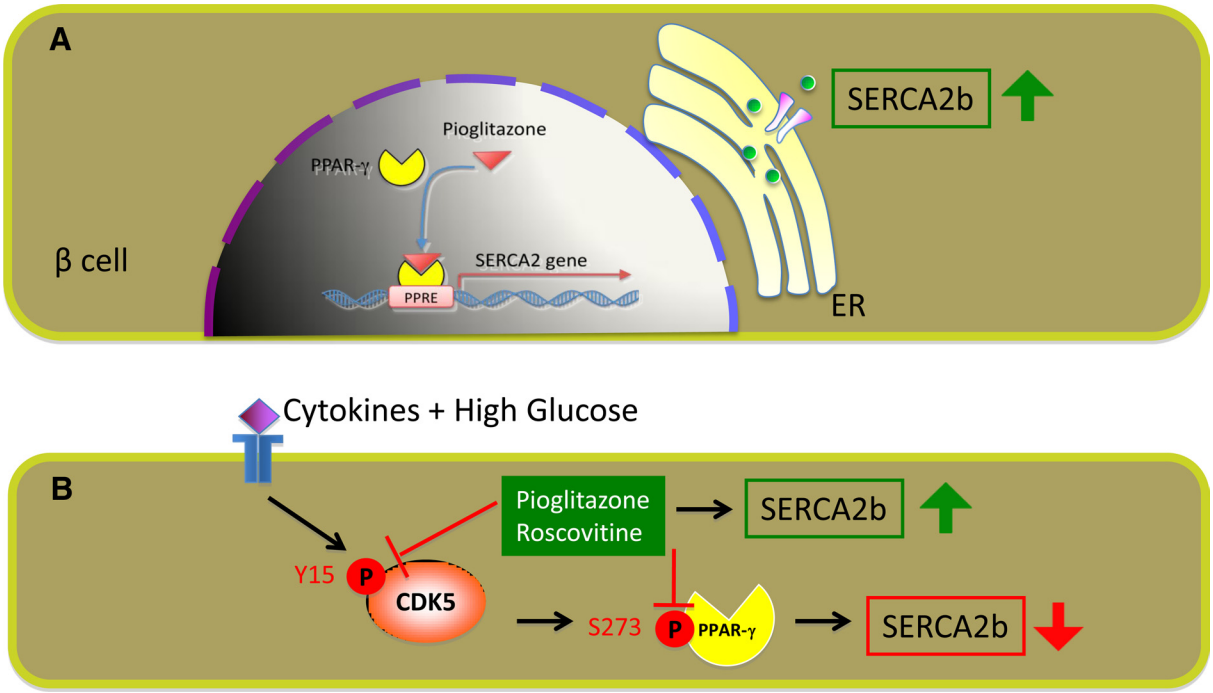

FIG. 10. Overall model. We propose that dysregulation of SERCA2b plays a prominent role in the progressive β-cell death and dysfunction observed in T2DM. Pharmacological activation of PPAR-γ has dual effects to preserve SERCA2b expression. First, PPAR-γ acts as a direct transcriptional regulator, and pharmacological activation with PPAR-γ ligands is expected to increase *SERCA2* gene transcription (panel A). Indirectly, pioglitazone preserves SERCA2b expression through inhibition of CDK5-mediated PPAR-γ phosphorylation (panel B). Pharmacological inhibition of CDK5 with roscovitine showed similar effects to prevent PPAR-γ phosphorylation and preserve SERCA2b expression levels. S273, Serine-273 and Y15, Tyrosine-15.

embedded, and sectioned at 5-μm intervals. Immunofluorescent analysis of insulin and SERCA2 was performed as previously described (26). Images were obtained using a Zeiss Z1 inverted microscope equipped with an Orca ER charge-coupled device camera (Hamamatsu Photonics, Hamamatsu City, Japan). Secondary antibodies were goat antirabbit IgG conjugated to Alexa Fluor 555 (1:200 dilution) and donkey antimouse conjugated to Alexa Fluor 488 (1:50 dilution) (Invitrogen).

Reporter assays

Deletion constructs of the human *SERCA2* promoter region were obtained as previously described and subcloned upstream of the luciferase coding sequence in the pGL3-basic plasmid (67). Mutagenesis of these constructs was performed using the Stratagene QuikChange Site-Directed Mutagenesis Kit (Agilent Technologies, Santa Clara, CA) according to the manufacturer's instructions. All sequences were confirmed by automated DNA sequencing. INS-1 cells were seeded in six-well plates 24 h before transfection. Plasmid (2 μg) diluted into 0.1 ml PBS was mixed with 6 μl of Metafectene Pro (Biotex, Munich, Germany) and incubated at room temperature for 15 min. The transfection mixture was added to each well of a six-well plate along with 2 ml of medium without antibiotics. At 6 h after transfection, the medium was replaced with fresh medium plus antibiotics with or without 10 μM pioglitazone. At 72 h after transfection, cells were harvested, and a luciferase assay was performed utilizing a commercially available luminometric kit (Promega Corp., Madison, WI). Luciferase activity was normalized to protein concentration as measured using the Bio-Rad Protein Assay reagent (Bio-Rad Laboratories, Inc., Hercules, CA) according to manufacturer's instructions. The dominant negative PPAR-γ construct in pcDNA3 was a kind gift of Dr. V. K. Chatterjee (Department of Medicine, University of Cambridge, Addenbrooke's Hospital, Cambridge CB2 2QQ, UK). Briefly, the construct was made by mutating the conserved hydrophobic and charged residues (Leu^{468} and Glu^{471}) in the putative AF-2 domain to alanine. The mutant receptor retains ligand and DNA binding but exhibits markedly reduced transactivation due to impaired coactivator recruitment (68).

ChIP assay

Approximately 2.5×10^7 INS-1 cells (from three confluent 10-cm dishes) were fixed in 1% formaldehyde for 15 min, sonicated to shear DNA fragments in the range of 800-2000 bp, and subjected to ChIP as detailed previously (66). Samples were quantitated in triplicate by SYBR Green I-based real-time PCR using forward and reverse primer sequences for the rat *SERCA2* promoter with the following sequences:

Forward: 5′-CGCTTTTGGCTGTGTGGGAAG-3′

Reverse: 5′-TGGTGTCCTTGGCTTGCCTC-3′. Immunoprecipitation with normal rabbit serum was performed as a negative control. As an additional negative control, PCR was performed to amplify *β-actin* genomic DNA using the ChIP-IT Control Kit for Rat (Active-Motif, Carlsbad, CA).

EMSA

EMSA was performed using the −55 to −24 fragment of the human *SERCA2* promoter containing the following sequence: 5′-GCGGCGGCGGCGAAAGGGGAGGCAGCGGCCGA-3′. A mutated probe was constructed with the following sequence: 5′-

GCGGCGGCTTCGAATTGGAGGCAGCGGCCGA-3′ Short oligonucleotide probes were generated by 5′ end-labeling single-stranded oligonucleotides with IRDye 232 800 (Li-Cor Biosciences). Labeled oligonucleotides were then annealed to an excess of 5′ end-labeled complementary strand. DNA-binding reactions (in 20 μl volumes) proceeded at room temperature as described previously (69) and consisted of 1 μg of INS-1 nuclear extract in a reaction buffer consisting of 10 mM HEPES (pH 7.9), 75 mM KCl, 2.5 mM $MgCl_2$, 0.1 mM EDTA, 1 mM dithiothreitol, 3% Ficoll, and 50 ng/liter polydeoxyinosinic deoxycytidylic acid. Reactions were subjected to electrophoresis on a 5% polyacrylamide gel. IRDye intensity was detected on the Odyssey infrared imaging system.

Overexpression experiments

A human SERCA2b expression vector containing a C-terminus Myc-DDK (FLAG) tag (Origene Technologies, Rockville, MD) was transfected into INS-1 832/13 cells using Lipofectamine 2000 reagent (Life Technologies, Gaithersburg, MD) according to the manufacturer's instructions. Briefly, logarithmically growing cells were transfected with 500 ng of plasmid and 2 μl of Lipofectamine 2000. At 72 h after transfection, GSIS assays were performed, and protein lysate was collected for immunoblotting.

GSIS

INS-1 cells were seeded in 12-well plates and allowed to reach 80–90% confluence. Cells were treated with 10 μM pioglitazone or DMSO for 16 h or transfected as described above. Cells were cultured an additional 6 h in the presence or absence of 5 ng/μl of IL-1β) and 25 mM glucose, and GSIS was performed as previously described (70). In brief, cells were preincubated in Hank's balanced salt solution (HBSS) (Life Technologies) with 2.5 mM glucose for 2 h and then switched to HBSS solution containing either 2.5 mM glucose or 15 mM glucose for an additional 2 h. Supernatants were collected and assayed for insulin levels using the Coat-A-Count insulin solid-phase RIA (Siemens Medical Solutions, Malvern, PA). Insulin secretion was normalized to the total protein of the cell extract.

Intracellular Ca^{2+} measurements

Semiconfluent INS-1 cells cultured in a 96-well plate were pretreated with or without pioglitazone for 16 h followed by combined treatment with IL-1β and 25 mM glucose for 24 h. Cells were then incubated in HBSS containing 2.5 mM glucose and 5 μM fura-2/AM (Invitrogen) for 30 min at 37 C in a CO_2 incubator. After rinsing, intracellular Ca^{2+}-dependent fluorescence was recorded using a SpectraMax M5 fluorescence imaging plate reader (Molecular Devices, Sunnyvale, CA). Fura-2 fluorescence was measured with excitation at 340 nm and 380 nm, and emission was measured at 510 nm. Human islets were cultured in a glass bottom dish (MatTek Corp., Ashland, MA), and incubation with fura-2/AM was performed in the same manner. The detection of intracellular Ca^{2+}-dependent fluorescence was performed as previously described (26) using a D1-fluorescent microscope (Zeiss, Oberkochen, Germany).

Statistical analysis

Differences between groups were examined for significance with either the two-tailed Student's *t* test or one-way ANOVA followed by the Tukey-Kramer posttest using GraphPad Prism statistics software (GraphPad Software, Inc., San Diego, CA). A P value < 0.05 was taken to indicate the presence of a significant difference.

Acknowledgments

We thank Shari Upchurch for her editorial assistance in preparing this manuscript.

Address all correspondence and requests for reprints to: Carmella Evans-Molina, Indiana University School of Medicine, 635 Barnhill Drive, MS 2031A, Indianapolis, Indiana 46202. E-mail: cevansmo@iupui.edu.

This work was supported by National Institutes of Health grants T32 HL079995 (to T.K.) and K08 DK080225, R03 DK 089147, and R01 DK093954 (to C.E.M.), an IUPUI DRIVE Award (to C.E.M.), and by Consejo Nacional de Ciencia y Tecnología grant 7850 and Programa de Apoyo a Proyectos de Investigación e Innovación Tecnológica grant IN204410 (to A.Z-H.). The funders had no role in study design, data collection and analysis, decision to publish, or preparation of the manuscript.

Disclosure Summary: T.K., G.A., D.R.M., L.G., A.Z.-H., Y.N., P.T.F., T.O., and C.E.M. have nothing to declare.

References

1. **Centers for Disease Control** 2011 National Diabetes Fact Sheet. www.cdc.gov/diabetes/pubs/pdf/ndfs_2011.pdf. Accessed 7–5-11
2. **World Health Organization** 2011 Diabetes Fact Sheet. www.who.int. Accessed 6–30-11
3. **Leahy JL** 2008 Mary, Mary, quite contrary, how do your β-cells fail? Diabetes 57:2563–2564
4. **Florez JC** 2008 Newly identified loci highlight β cell dysfunction as a key cause of type 2 diabetes: where are the insulin resistance genes? Diabetologia 51:1100–1110
5. **Butler AE, Janson J, Bonner-Weir S, Ritzel R, Rizza RA, Butler PC** 2003 β-Cell deficit and increased β-cell apoptosis in humans with type 2 diabetes. Diabetes 52:102–110
6. **Festa A, Williams K, D'Agostino Jr R, Wagenknecht LE, Haffner SM** 2006 The natural course of β-cell function in nondiabetic and diabetic individuals: the Insulin Resistance Atherosclerosis Study. Diabetes 55:1114–1120
7. **Turner RC, Cull CA, Frighi V, Holman RR** 1999 Glycemic control with diet, sulfonylurea, metformin, or insulin in patients with type 2 diabetes mellitus: progressive requirement for multiple therapies (UKPDS 49). UK Prospective Diabetes Study (UKPDS) Group. JAMA 281:2005–2012
8. **Eizirik DL, Cardozo AK, Cnop M** 2008 The role for endoplasmic reticulum stress in diabetes mellitus. Endocr Rev 29:42–61
9. **Robertson R, Zhou H, Zhang T, Harmon JS** 2007 Chronic oxidative stress as a mechanism for glucose toxicity of the β cell in type 2 diabetes. Cell Biochem Biophys 48:139–146
10. **Robertson RP** 2009 β-cell deterioration during diabetes: what's in the gun? Trends Endocrinol Metab 20:388–393
11. **Gupta D, Kono T, Evans-Molina C** 2010 The role of peroxisome proliferator-activated receptor γ in pancreatic β cell function and survival: therapeutic implications for the treatment of type 2 diabetes mellitus. Diabetes Obes Metab 12:1036–1047
12. **Guest PC, Bailyes EM, Hutton JC** 1997 Endoplasmic reticulum Ca^{2+} is important for the proteolytic processing and intracellular

transport of proinsulin in the pancreatic β-cell. Biochem J 323:445–450
13. **Drews G, Krippeit-Drews P, Düfer M** 2010 Electrophysiology of islet cells. Adv Exp Med Biol 654:115–163
14. **Tarasov A, Dusonchet J, Ashcroft F** 2004 Metabolic regulation of the pancreatic β-cell ATP-sensitive K+ channel: a pas de deux. Diabetes 53(Suppl 3):S113–S122
15. **Lang J** 1999 Molecular mechanisms and regulation of insulin exocytosis as a paradigm of endocrine secretion. Eur J Biochem 259: 3–17
16. **Lodish HF, Kong N** 1990 Perturbation of cellular calcium blocks exit of secretory proteins from the rough endoplasmic reticulum. J Biol Chem 265:10893–10899
17. **Pena F, Jansens A, van Zadelhoff G, Braakman I** 2010 Calcium as a crucial cofactor for low density lipoprotein receptor folding in the endoplasmic reticulum. J Biol Chem 285:8656–8664
18. **Meldolesi J, Pozzan T** 1998 The endoplasmic reticulum Ca^{2+} store: a view from the lumen. Trends Biochem Sci 23:10–14
19. **Bygrave FL, Benedetti A** 1996 What is the concentration of calcium ions in the endoplasmic reticulum? Cell Calcium 19:547–551
20. **Miyawaki A, Llopis J, Heim R, McCaffery JM, Adams JA, Ikura M, Tsien RY** 1997 Fluorescent indicators for Ca^{2+} based on green fluorescent proteins and calmodulin. Nature 388:882–887
21. **Moore CE, Omikorede O, Gomez E, Willars GB, Herbert TP** 2011 PERK Activation at low glucose concentration is mediated by SERCA pump inhibition and confers preemptive cytoprotection to pancreatic β-cells. Mol Endocrinol 25:315–326
22. **Toyoshima C, Nakasako M, Nomura H, Ogawa H** 2000 Crystal structure of the calcium pump of sarcoplasmic reticulum at 2.6 A resolution. Nature 405:647–655
23. **Dally S, Corvazier E, Bredoux R, Bobe R, Enouf J** 2010 Multiple and diverse coexpression, location, and regulation of additional SERCA2 and SERCA3 isoforms in nonfailing and failing human heart. J Mol Cell Cardiol 48:633–644
24. **Hovnanian A** 2007 SERCA pumps and human diseases. Subcell Biochem 45:337–363
25. **Chen L, Koh DS, Hille B** 2003 Dynamics of calcium clearance in mouse pancreatic β-cells. Diabetes 52:1723–1731
26. **Evans-Molina C, Robbins RD, Kono T, Tersey SA, Vestermark GL, Nunemaker CS, Garmey JC, Deering TG, Keller SR, Maier B, Mirmira RG** 2009 PPAR-γ activation restores islet function in diabetic mice through reduction of ER stress and maintenance of euchromatin structure. Mol Cell Biol 29:2053–2067
27. **Roe MW, Philipson LH, Frangakis CJ, Kuznetsov A, Mertz RJ, Lancaster ME, Spencer B, Worley III JF, Dukes ID** 1994 Defective glucose-dependent endoplasmic reticulum Ca^{2+} sequestration in diabetic mouse islets of Langerhans. J Biol Chem 269:18279–18282
28. **Cardozo AK, Ortis F, Storling J, Feng YM, Rasschaert J, Tonnesen M, Van Eylen F, Mandrup-Poulsen T, Herchuelz A, Eizirik DL** 2005 Cytokines downregulate the sarcoendoplasmic reticulum pump Ca^{2+} ATPase 2b and deplete endoplasmic reticulum Ca^{2+}, leading to induction of endoplasmic reticulum stress in pancreatic β-cells. Diabetes 54:452–461
29. **Like AA, Rossini AA** 1976 Streptozotocin-induced pancreatic insulitis: new model of diabetes mellitus. Science 193:415–417
30. **Crosby MB, Svenson J, Gilkeson GS, Nowling TK** 2005 A novel PPAR response element in the murine iNOS promoter. Mol Immunol 42:1303–1310
31. **Gupta D, Jetton TL, Mortensen RM, Duan SZ, Peshavaria M, Leahy JL** 2008 In vivo and in vitro studies of a functional peroxisome proliferator-activated receptor γ response element in the mouse pdx-1 promoter. J Biol Chem 283:32462–32470
32. **Gupta D, Peshavaria M, Monga N, Jetton TL, Leahy JL** 2010 Physiologic and pharmacologic modulation of glucose-dependent insulinotropic polypeptide (GIP) receptor expression in β-cells by peroxisome proliferator-activated receptor (PPAR)-γ signaling: possible mechanism for the GIP resistance in type 2 diabetes. Diabetes 59:1445–1450
33. **Kim HI, Kim JW, Kim SH, Cha JY, Kim KS, Ahn YH** 2000 Identification and functional characterization of the peroxisomal proliferator response element in rat GLUT2 promoter. Diabetes 49: 1517–1524
34. **Lemay DG, Hwang DH** 2006 Genome-wide identification of peroxisome proliferator response elements using integrated computational genomics. J Lipid Res 47:1583–1587
35. **Schachtrup C, Emmler T, Bleck B, Sandqvist A, Spener F** 2004 Functional analysis of peroxisome-proliferator-responsive element motifs in genes of fatty acid-binding proteins. Biochem J 382:239–245
36. **Venkatachalam G, Kumar AP, Yue LS, Pervaiz S, Clement MV, Sakharkar MK** 2009 Computational identification and experimental validation of PPRE motifs in NHE1 and MnSOD genes of human. BMC Genomics 10(Suppl 3):S5
37. **Boni-Schnetzler M, Ehses JA, Faulenbach M, Donath MY** 2008 Insulitis in type 2 diabetes. Diabetes Obes Metab 10(Suppl 4):201–204
38. **Böni-Schnetzler M, Thorne J, Parnaud G, Marselli L, Ehses JA, Kerr-Conte J, Pattou F, Halban PA, Weir GC, Donath MY** 2008 Increased interleukin (IL)-1β messenger ribonucleic acid expression in β-cells of individuals with type 2 diabetes and regulation of IL-1β in human islets by glucose and autostimulation. J Clin Endocrinol Metab 93:4065–4074
39. **Ehses JA, Perren A, Eppler E, Ribaux P, Pospisilik JA, Maor-Cahn R, Gueripel X, Ellingsgaard H, Schneider MK, Biollaz G, Fontana A, Reinecke M, Homo-Delarche F, Donath MY** 2007 Increased number of islet-associated macrophages in type 2 diabetes. Diabetes 56:2356–2370
40. **Larsen CM, Faulenbach M, Vaag A, Volund A, Ehses JA, Seifert B, Mandrup-Poulsen T, Donath MY** 2007 Interleukin-1-receptor antagonist in type 2 diabetes mellitus. N Engl J Med 356:1517–1526
41. **Dinarello CA, Donath MY, Mandrup-Poulsen T** 2010 Role of IL-1β in type 2 diabetes. Curr Opin Endocrinol Diabetes Obes 17:314–321
42. **Choi JH, Banks AS, Estall JL, Kajimura S, Boström P, Laznik D, Ruas JL, Chalmers MJ, Kamenecka TM, Blüher M, Griffin PR, Spiegelman BM** 2010 Anti-diabetic drugs inhibit obesity-linked phosphorylation of PPARγ by Cdk5. Nature 466:451–456
43. **Morigaki R, Sako W, Okita S, Kasahara J, Yokoyama H, Nagahiro S, Kaji R, Goto S** 2011 Cyclin-dependent kinase 5 with phosphorylation of tyrosine 15 residue is enriched in striatal matrix compartment in adult mice. Neuroscience 189:25–31
44. **Hisanaga S, Endo R** 2010 Regulation and role of cyclin-dependent kinase activity in neuronal survival and death. J Neurochem 115: 1309–1321
45. **Vandecaetsbeek I, Trekels M, De Maeyer M, Ceulemans H, Lescrinier E, Raeymaekers L, Wuytack F, Vangheluwe P** 2009 Structural basis for the high Ca^{2+} affinity of the ubiquitous SERCA2b Ca^{2+} pump. Proc Natl Acad Sci USA 106:18533–18538
46. **Arredouani A, Guiot Y, Jonas JC, Liu LH, Nenquin M, Pertusa JA, Rahier J, Rolland JF, Shull GE, Stevens M, Wuytack F, Henquin JC, Gilon P** 2002 SERCA3 ablation does not impair insulin secretion but suggests distinct roles of different sarcoendoplasmic reticulum Ca^{2+} pumps for Ca^{2+} homeostasis in pancreatic β-cells. Diabetes 51:3245–3253
47. **Ravier MA, Daro D, Roma LP, Jonas JC, Cheng-Xue R, Schuit FC, Gilon P** 2011 Mechanisms of control of the free Ca^{2+} concentration in the endoplasmic reticulum of mouse pancreatic β-cells: interplay with cell metabolism and $[Ca^{2+}]c$ and role of SERCA2b and SERCA3. Diabetes 60:2533–2545
48. **Meijer L, Borgne A, Mulner O, Chong JP, Blow JJ, Inagaki N, Inagaki M, Delcros JG, Moulinoux JP** 1997 Biochemical and cellular effects of roscovitine, a potent and selective inhibitor of the

cyclin-dependent kinases cdc2, cdk2 and cdk5. Eur J Biochem 243: 527–536

49. **Chistiakov DA, Potapov VA, Smetanina SA, Bel'chikova LN, Suplotova LA, Nosikov VV** 2011 The carriage of risk variants of CDKAL1 impairs beta-cell function in both diabetic and non-diabetic patients and reduces response to non-sulfonylurea and sulfonylurea agonists of the pancreatic KATP channel. Acta Diabetol 48:227–235
50. **Haupt A, Staiger H, Schäfer SA, Kirchhoff K, Guthoff M, Machicao F, Gallwitz B, Stefan N, Häring HU, Fritsche A** 2009 The risk allele load accelerates the age-dependent decline in β cell function. Diabetologia 52:457–462
51. **Hu C, Zhang R, Wang C, Wang J, Ma X, Lu J, Qin W, Hou X, Wang C, Bao Y, Xiang K, Jia W** 2009 PPARG, KCNJ11, CDKAL1, CDKN2A-CDKN2B, IDE-KIF11-HHEX, IGF2BP2 and SLC30A8 are associated with type 2 diabetes in a Chinese population. PLoS One 4:e7643
52. **Ching YP, Pang AS, Lam WH, Qi RZ, Wang JH** 2002 Identification of a neuronal Cdk5 activator-binding protein as Cdk5 inhibitor. J Biol Chem 277:15237–15240
53. **Lee HY, Jung H, Jang IH, Suh PG, Ryu SH** 2008 Cdk5 phosphorylates PLD2 to mediate EGF-dependent insulin secretion. Cell Signal 20:1787–1794
54. **Lilja L, Johansson JU, Gromada J, Mandic SA, Fried G, Berggren PO, Bark C** 2004 Cyclin-dependent kinase 5 associated with p39 promotes Munc18–1 phosphorylation and Ca^{2+}-dependent exocytosis. J Biol Chem 279:29534–29541
55. **Lilja L, Yang SN, Webb DL, Juntti-Berggren L, Berggren PO, Bark C** 2001 Cyclin-dependent kinase 5 promotes insulin exocytosis. J Biol Chem 276:34199–34205
56. **Wei FY, Nagashima K, Ohshima T, Saheki Y, Lu YF, Matsushita M, Yamada Y, Mikoshiba K, Seino Y, Matsui H, Tomizawa K** 2005 Cdk5-dependent regulation of glucose-stimulated insulin secretion. Nat Med 11:1104–1108
57. **Kitani K, Oguma S, Nishiki T, Ohmori I, Galons H, Matsui H, Meijer L, Tomizawa K** 2007 A Cdk5 inhibitor enhances the induction of insulin secretion by exendin-4 both in vitro and in vivo. J Physiol Sci 57:235–239
58. **Ubeda M, Rukstalis JM, Habener JF** 2006 Inhibition of cyclin-dependent kinase 5 activity protects pancreatic β cells from glucotoxicity. J Biol Chem 281:28858–28864
59. **Zheng YL, Hu YF, Zhang A, Wang W, Li B, Amin N, Grant P, Pant HC** 2010 Overexpression of p35 in Min6 pancreatic β cells induces a stressed neuron-like apoptosis. J Neurol Sci 299:101–107
60. **Camins A, Verdaguer E, Folch J, Canudas AM, Pallàs M** 2006 The role of CDK5/P25 formation/inhibition in neurodegeneration. Drug News Perspect 19:453–460
61. **Hamdane M, Buée L** 2007 The complex p25/Cdk5 kinase in neurofibrillary degeneration and neuronal death: the missing link to cell cycle. Biotechnol J 2:967–977
62. **Piedrahita D, Hernández I, López-Tobón A, Fedorov D, Obara B, Manjunath BS, Boudreau RL, Davidson B, Laferla F, Gallego-Gómez JC, Kosik KS, Cardona-Gómez GP** 2010 Silencing of CDK5 reduces neurofibrillary tangles in transgenic alzheimer's mice. J Neurosci 30:13966–13976
63. **Daval M, Gurlo T, Costes S, Huang CJ, Butler PC** 2011 Cyclin-dependent kinase 5 promotes pancreatic β-cell survival via Fak-Akt signaling pathways. Diabetes 60:1186–1197
64. **Gotoh M, Maki T, Kiyoizumi T, Satomi S, Monaco AP** 1985 An improved method for isolation of mouse pancreatic islets. Transplantation 40:437–438
65. **Evans-Molina C, Garmey JC, Ketchum R, Brayman KL, Deng S, Mirmira RG** 2007 Glucose regulation of insulin gene transcription and pre-mRNA processing in human islets. Diabetes 56:827–835
66. **Chakrabarti SK, James JC, Mirmira RG** 2002 Quantitative assessment of gene targeting in vitro and in vivo by the pancreatic transcription factor, Pdx1. Importance of chromatin structure in directing promoter binding. J Biol Chem 277:13286–13293
67. **Zarain-Herzberg A, Alvarez-Fernández G** 2002 Sarco(endo)plasmic reticulum Ca^{2+}-ATPase-2 gene: structure and transcriptional regulation of the human gene. ScientificWorldJournal 2:1469–1483
68. **Gurnell M, Wentworth JM, Agostini M, Adams M, Collingwood TN, Provenzano C, Browne PO, Rajanayagam O, Burris TP, Schwabe JW, Lazar MA, Chatterjee VK** 2000 A dominant-negative peroxisome proliferator-activated receptor gamma (PPARγ) mutant is a constitutive repressor and inhibits PPARγ-mediated adipogenesis. J Biol Chem 275:5754–5759
69. **Ohneda K, Mirmira RG, Wang J, Johnson JD, German MS** 2000 The homeodomain of PDX-1 mediates multiple protein-protein interactions in the formation of a transcriptional activation complex on the insulin promoter. Mol Cell Biol 20:900–911
70. **Hohmeier HE, Mulder H, Chen G, Henkel-Rieger R, Prentki M, Newgard CB** 2000 Isolation of INS-1-derived cell lines with robust ATP-sensitive K+ channel-dependent and -independent glucose-stimulated insulin secretion. Diabetes 49:424–430